Illumination compensation and normalization in eigenspace-based face recognition: A comparative study of different pre-processing approaches

Javier Ruiz-del-Solar *, Julio Quinteros

Department of Electrical Engineering, Universidad de Chile, Avenida Tupper 2007, Casilla, 412-3 Santiago, Chile

ABSTRACT

The aim of this work is to investigate illumination compensation and normalization in eigenspace-based face recognition by carrying out an independent comparative study among several pre-processing algorithms. This research is motivated by the lack of direct and detailed comparisons of those algorithms in equal working conditions. The results of this comparative study intend to be a guide for the developers of face recognitions systems. The study focuses on algorithms with the following properties: (i) general purpose, (ii) no modeling steps or training images required, (iii) simplicity, (iv) high speed, and (v) high performance in terms of recognition rates. Thus, herein five different algorithms are compared, by using them as a pre-processing stage in 16 different eigenspace-based face recognition systems. The comparative study is carried out in a face identification scenario using a large amount of images from the PIE, Yale B and Notre Dame face databases. As a result of this study we concluded that the most suitable algorithms for achieving illumination compensation and normalization in eigenspace-based face recognition are SQI and the modified LBP transform.

1. Introduction

Variable illumination is one of the most important problems in face recognition. The main reason is the fact that illumination, together with pose variation, is the most significant factor that alters the perception (appearance) of faces (Gross et al., 2004; Shin et al., 2008). Lighting conditions change largely between indoor and outdoor environments, but also within indoor environments. Thus, due to the 3D shape of human faces, a direct lighting source can produce strong shadows that accentuate or diminish certain facial features. Moreover, extreme lighting can produce too dark or too bright images, which can disturb the recognition process (Basri and Jacobs, 2004). Although, the ability of algorithms to recognize faces across illumination changes has made important progress in the last years, FRVT 2006 results show that illumination still has an important effect on the recognition process (Phillips et al., 2007).

Several approaches have been proposed in the last years for solving the variable illumination problem in face recognition contexts (Pizer et al., 1987; Adini et al., 1997; Belhumeur and Kriegman, 1998; Chen et al., 2000, 2006; Georghiades et al., 2001; Shashua and Riklin-Raviv, 2001; Ramamoorthi, 2002; Gross and Brajovic, 2003; Shan et al., 2003; Sim et al., 2003; Zhang and Samaras, 2003; Zhao et al., 2003; Ahonen et al., 2004; Fröba and Ernst, 2004; Gross et al., 2004; Short et al., 2004; Wang et al., 2004; Lee

et al., 2005; Zhang et al., 2005; Xie and Lam, 2006; Shin et al., 2008; just no name a few). These approaches can be roughly classified into three main categories: *face modeling, normalization and pre-processing*, and *invariant features extraction*.

Face modeling approaches use low-dimensional linear subspaces for modeling image variations of human faces under different lighting conditions. As an example, the illumination cone method (Belhumeur and Kriegman, 1998; Georghiades et al., 2001) exploits the fact that the set of images of an object (a face) in fixed pose, but under all possible illumination conditions, forms a convex cone in the images' space. Illumination cones of human faces can be approximated by low-dimensional linear subspaces whose basis vectors are estimated using a generative model. The generative model is built using a small number of training images of each face, taken using different lighting directions. The recognition algorithm assigns to a test image the identity of the closest illumination cone. Similarly, in the spherical harmonic method (Ramamoorthi, 2002) it is analyzed the subspace best approximating images of a convex Lambertian object, taken from the same viewpoint, but under different distant illumination conditions. Principal component analysis (PCA) is applied, and a low-dimensional (less than nine-dimensional) approximation of illumination cones is obtained. One of main drawbacks of the face modeling approaches is the requirement of images for building the linear subspaces. This drawback limits its application in practical problems. Lee et al. (2005) show how to arrange physical lighting so that the acquired images of each object can be directly used as basis images of the

* Corresponding author. Fax: +56 2 695 3881.
E-mail address: jruizd@ing.uchile.cl (J. Ruiz-del-Solar).

linear subspaces. However, it still remains the requirement of images for building the models. Moreover, the specularity problem and the fact that human faces are not perfect Lambertian surfaces are ignored by these models (Chen et al., 2006).

In the second category, *normalization and preprocessing*, image pre-processing algorithms are employed to compensate and normalize illumination. Most of these algorithms do not require any training or modeling steps, knowledge of 3D face models or reflective surface models. For instance, in (Shashua and Riklin-Raviv, 2001) is proposed the quotient image (QI) method, which is a practical algorithm for extracting an illumination-normalized representation of an image (e.g., face image). The QI, defined as the ratio between a test image and linear combinations of three non-coplanar illuminated images, depends only on the Albedo information, which is illumination free. In (Wang et al., 2004) is introduced the self-quotient image (SQI), which corresponds to the ratio between a test image and a smoothed version of it. The main improvement of SQI over QI is the fact that it needs only one image for extracting the intrinsic lighting properties of the image. Using just one image means also that no image alignment is required. Moreover, SQI works properly also in shadow regions. Similarly, Gross and Brajovic (2003) proposed a pre-processing algorithm that also consists in extracting the Albedo information using the ratio between a test image and a second image, which corresponds to an estimation of the illumination field. This last image is obtained directly from the test image, and as in the SQI algorithm no image alignment is required, and the method works properly in shadow regions. Xie and Lam (2006) proposed a related approach, in which the intensity of the pixels is locally normalized (zero-mean and unit variance) using a 7×7 window centered at the pixel. The method is based on two assumptions: (i) in a small image region W, the surface normal direction can be considered constant, and (ii) the light source is directional, and therefore, from (i) and (ii), almost constant in W. Another interesting algorithm is the so-called plane subtraction or illumination gradient compensation algorithm (Sung and Poggio, 1998; Ruiz-del-Solar and Navarrete, 2005), which consists on calculating a best-fit brightness plane to the image under analysis, and then subtracting this plane to the image. This method allows compensating heavy shadows caused by extreme lighting angles. In addition to the mentioned algorithms, general-purpose image pre-processing algorithms such as histogram equalization, Gamma correction, and logarithmic transforms have also been used for illumination normalization (Pizer et al., 1987; Shan et al., 2003; Ruiz-del-Solar and Navarrete, 2005). In the specific case of PCA-based face recognition, some authors suggest that illumination normalization can be achieved by discarding the first three PCA components.

In the third category, *invariant features extraction*, illumination invariant features are extracted and face recognition is carried out using these features. Thus, in (Adini et al., 1997) edge maps, images convolved with 2D Gabor-like filters, and image intensity derivatives are employed as illumination invariant representations. The main conclusion of that study is that those image representations are insufficient by themselves to overcome variations because of changes in illumination direction. Very recently the discrete cosine transform (DCT) was proposed for compensating illumination variations in the logarithmic domain (Chen et al., 2006). Taking into account that illumination variations mainly lie in the low-frequency band, the main idea is to discard DCT coefficients corresponding to low-level frequencies. The obtained results are very promissory, although important issues such as the relation between the number of selected DCT coefficients, the size of the images, and the cutoff frequency, are not detailed addressed. Another invariant transform is the LBP (local binary pattern) (Ojala et al., 1996), which allows compensating illumination using a local-contrast based image representation. This transform and its

extension, known as modified LBP, have been employed to compensate and normalize illumination in face detection (Fröba and Ernst, 2004) and face recognition (Ahonen et al., 2004) contexts.

Thus, the aim of this work is to investigate illumination compensation and normalization in eigenspace-based face recognition by carrying out an independent comparative study among several pre-processing algorithms. This research is motivated by the lack of direct and detailed comparisons of those algorithms in equal working conditions. The results of this comparative study intend to be a guide for the developers of face recognitions systems. We concentrate ourselves in algorithms with the following properties: (i) general purpose, (ii) no modeling steps or training images required, (iii) simplicity, (iv) high speed, and (v) high performance in terms of recognition rates. The high speed requirement is important in our case, because we are especially interested in the construction of real-time human-computer interfaces. The selected algorithms to be compared belong to the *normalization and pre-processing* category: SQI, Gross and Barjovic' pre-processing algorithm, and plane subtraction with histogram equalization, and to the *invariant features extraction* category: LBP and modified LBP.

The comparative study is carried out using eienspace-based face recognition systems, mainly because this family of face recognition methods is by far the most used one. Eigenspace-based methods, mostly derived from the eigenspace-algorithm (Turk and Pentland, 1991), project input faces onto a dimensional reduced space where the recognition is carried out, performing a holistic analysis of the faces. Different eigenspace-based methods have been proposed. They differ mostly in the kind of projection/decomposition approach used (standard-, differential- or Kernel–Eigenspace), in the projection algorithm been employed, in the use of simple or differential images before/after projection, and in the similarity matching criterion or classification method employed (see Ruiz-del-Solar and Navarrete, 2005 for an overview of all these different methods). In this study we consider 16 different face recognition systems, which are built using four different projections methods (principal component analysis – (PCA), Fisher linear discriminant – (FLD), Kernel PCA – KPCA and Kernel–Fisher discriminant – (KFD)) and four different similarity measures (Euclidean-, Mahalanobis-, Cosines- and Whitening-Cosines-distance). The study is carried out in two stages. In the first stage the five illumination compensation and normalization algorithms are used as a pre-processing stage in each of these 16 face recognition systems. The algorithms are compared and analyzed using a large amount of images from two face databases, PIE (PIE Database, 2006) and Yale B (Yale Face Database B, 2006), which contains face images with very different illumination conditions. As a result of these experiments, the algorithms with the best illumination compensation and normalization capabilities are selected for a deeper analysis. In the second stage the selected algorithms are compared using the Notre Dame database (Flynn et al., 2003), and four face recognition systems. In this second set of experiments larger probe and gallery sets, in terms of individuals, are employed, and the statistical significance of the tests is analyzed. In both stages the algorithms are evaluated in a face identification scenario; face verification or watch-list search are not considered.

This study corresponds to an extension of the one presented in (Ruiz-del-Solar and Navarrete, 2005), where illumination compensation and normalization was not addressed. We believe that carrying out independent comparative studies between different recognition algorithms is relevant, because comparisons are in general performed using the own implementations of the research groups that have proposed each method, which does not consider completely equal working conditions. Very often, more than a comparison between the capabilities of the algorithms, a contest between the abilities of the research groups is performed.

Additionally, not all the possible implementations are considered, but only the ones that some groups have decided to use.

This paper is structured as follows: The five algorithms under analysis are described in Section 2. In Section 3 a comparative study among these algorithms is presented. Finally, conclusions of this work are given in Section 4.

2. Illumination compensation and normalization algorithms under comparison

2.1. Illumination plane subtraction with histogram equalization

The illumination plane $\mathbf{IP}(x,y)$ of an image $\mathbf{I}(x,y)$ corresponds to the best-fit plane from the image intensities. $\mathbf{IP}(x,y)$ is a linear approximation of $\mathbf{I}(x,y)$, given by

$$\mathbf{IP}(x,y) = a \cdot x + b \cdot y + c \tag{1}$$

The plane parameters a, b and c can be estimated by the linear regression formula:

$$\mathbf{p} = (\mathbf{N}^T\mathbf{N})^{-1}\mathbf{N}^T\mathbf{x} \tag{2}$$

where $\mathbf{p} \in \Re^3$ is a vector containing the plane parameters (a, b and c) and $\mathbf{x} \in \Re^n$ is $\mathbf{I}(x,y)$ in vector form (n is the number of pixels). $\mathbf{N} \in \Re^{n \times 3}$ is a matrix containing the pixel coordinates: the first column contains the horizontal coordinates, the second column the vertical coordinates, and the third column has all its values set to 1.

After estimating $\mathbf{IP}(x,y)$, this plane is subtracted from $\mathbf{I}(x,y)$. This allows reducing shadows caused by extreme lighting angles. Afterward, histogram equalization is applied for compensating changes in illumination brightness, and differences in camera response curves. Some example images obtained after applying plane subtraction (PS) and histogram equalization (HE) are shown in Figs. 1c–d and 2c–d. Plane subtraction together with histogram equalization was applied in (Sung and Poggio, 1998) for face detection purposes, and in (Ruiz-del-Solar and Navarrete, 2005) for obtaining illumination compensation in face recognition. In this last case, histogram equalization is followed by intensity normalization of the face vectors (zero-mean and unit variance).

2.2. Self-quotient image

The self-quotient image (SQI) method is based on the reflectance illumination model of the human vision (Retinex theory: Land, 1977; Jobson et al., 1996), which assumes: (i) human vision is mostly sensitive to scene reflectance and mostly insensitive to the illumination conditions, and (ii) human vision responds to local changes in contrast, rather than to global brightness levels. These two assumptions are related because local contrast is a function of the reflectance. Thus, the reflectance is given by

$$I(x,y)\frac{1}{L(x,y)} = R(x,y) \tag{3}$$

with $I(x,y)$ the input stimulus (in this case the input image), and $L(x,y)$ the illuminance or perception gain at each point.

Illuminance can be considered as the low-frequency component of the input stimulus, as has been proved by the spherical harmonics analysis (Ramamoorthi, 2002). Then, illuminance can be estimated as

$$L(x,y) \approx F(x,y) * I(x,y) \tag{4}$$

with $F(x,y)$ a low-pass filter.

From (3) to (4) the self-quotient image $Q(x,y)$ is defined as

$$Q(x,y) = \frac{I(x,y)}{F(x,y) * I(x,y)} \approx R(x,y) \tag{5}$$

It should be noted that the properties of $Q(x,y)$ are dependant on the kernel size of $F(x,y)$. If too small, then $Q(x,y)$ will approximate one, and the Albedo information will be lost; if too large, there will appear halo effects near edges. In (Wang et al., 2004) this problem is solved by using a multi-scale technique that employs kernels of variable size. Another important improvement is the use of weighting kernels that divide the convolution windows in two different regions, depending on the observed pixel intensities. This technique is supposed to avoid halo effects near the edges. Thus, the final SQI computation procedure is given by (see Wang et al., 2004 for details):

(1) Select several smoothing Gaussian kernels $G_1,\ldots,G_n$, calculate the corresponding weighting kernels $W_1,\ldots,W_n$, and the resulting multi-scale self-quotient images as

$$Q_k(x,y) = \frac{I(x,y)}{I(x,y) * \left(\frac{1}{N}W_kG_k\right)}, \quad k = 1,\ldots,n \tag{6}$$

N is a normalization factor for obtaining normalized kernels W_kG_k.

(2) Summarize the multi-scale self-quotient images, after applying to each one a non-linear function T (Arctangent or Sigmoid)

$$Q(x,y) = \sum_{k=1}^{n} m_k T(Q_k(x,y)) \tag{7}$$

m_k are weighting factors (usually set to one). Some example images obtained after applying SQI are shown in Figs. 1e and 2e.

2.3. Gross and Brajovic' preprocessing algorithm

The pre-processing algorithm proposed by Gross and Brajovic (2003) is also based on the reflectance illumination model of the human vision described in the former section. In this case the reflectance is computed as

$$I(x,y)\frac{1}{I_\psi(x,y)} = R(x,y), \quad (x,y) \in \psi \tag{8}$$

where $I_\psi(x,y)$ is the stimulus level in a small neighborhood ψ in the input image.

It can be seen that (8) is similar to (5). The difference in both methods is the way in which the denominator term is computed. In (Gross and Brajovic, 2003) $I_\psi(x,y) = L(x,y)$ is computed by regularization, and by imposing a smoothness constraint in this computation. The final discretized, linear partial differential equation to be solved becomes:

$$L_{i,j} + \frac{\lambda}{h}\left[\frac{1}{\rho_{i,j-1/2}}(L_{i,j} - L_{i,j-1}) + \frac{1}{\rho_{i,j+1/2}}(L_{i,j} - L_{i,j+1}) + \frac{1}{\rho_{i-1/2,j}}(L_{i,j} - L_{i-1,j})\right.$$
$$\left. + \frac{1}{\rho_{i+1/2,j}}(L_{i,j} - L_{i+1,j})\right] = I \tag{9}$$

with λ a parameter that controls the relative importance of the terms, h the pixel grid size, and ρ a varying permeability weight that controls the anisotropic nature of the smoothing constraint. In (Gross and Brajovic, 2003) are given the details on how to solve (9). In this work this algorithm will be named as SIP (Shadow Illuminator Pro), which is the name of a commercial program that implements it, and that will be used in this study. Some example images obtained after applying the SIP algorithm are shown in Figs. 1f–g and 2f–g.

Fig. 1. Example image of an individual from the Yale B database (a). The image is pre-processed by masking the central part (b). Afterwards several illumination invariant algorithms are applied (c–i). PS: illumination plane subtraction; HE: histogram equalization; SQI: self-quotient image; SIP: Gross and Brajovic' algorithm implemented by Shadow Illuminator Pro; LBP: local binary pattern; mLBP: modified LBP. See Section 3.2 for details.

2.4. Local binary pattern (LBP)

The local binary pattern (LBP), introduced originally for texture description in (Ojala et al., 1996), has been used in the last years to compensate and normalize illumination in face detection and recognition contexts. LBP, also known as census transform (Zabih and Woodfill, 1994), is defined as an ordered set of pixel intensity comparisons, in a local neighborhood $N(x_c, y_c)$, which represents those pixels having a lower intensity than the center pixel $I(x_c, y_c)$. In other words, LBP generates a string of bits representing which pixels in $N(x_c, y_c)$ have a lower intensity than $I(x_c, y_c)$. $I(x_c, y_c)$ is not included in $N(x_c, y_c)$. Formally speaking let a comparison function

$\mathbf{h}(I(x_c, y_c), I(x, y))$ be 1 if $I(x_c, y_c) < I(x, y)$ and 0 otherwise. Then, the LBP is defined as

$$LBP(x, y) = \bigcup_{(x', y') \in N(x, y)} h(I(x, y), I(x', y')) \qquad (10)$$

with $\cup$ the concatenation operator. Normally, a neighborhood of 3×3 pixels is used, although larger neighborhood can be defined (Ahonen et al., 2004). In the case of a 3×3 neighborhood, $LBP(x, y)$ corresponds to the concatenation of 8 bits. LBP transforms images in illumination invariant feature representations (see Figs. 1h and 2h), because all its computations are local, and they depend on the relative values between neighbor pixels (local contrast).

(a) Original   (b) Masked (M)   (c) M+PS   (d) M+PS+H

(e) M+SQI-2D   (f) M+SIP-77-62   (g) M+SIP-100-90   (h) M+LBP

(i) M+mLBP
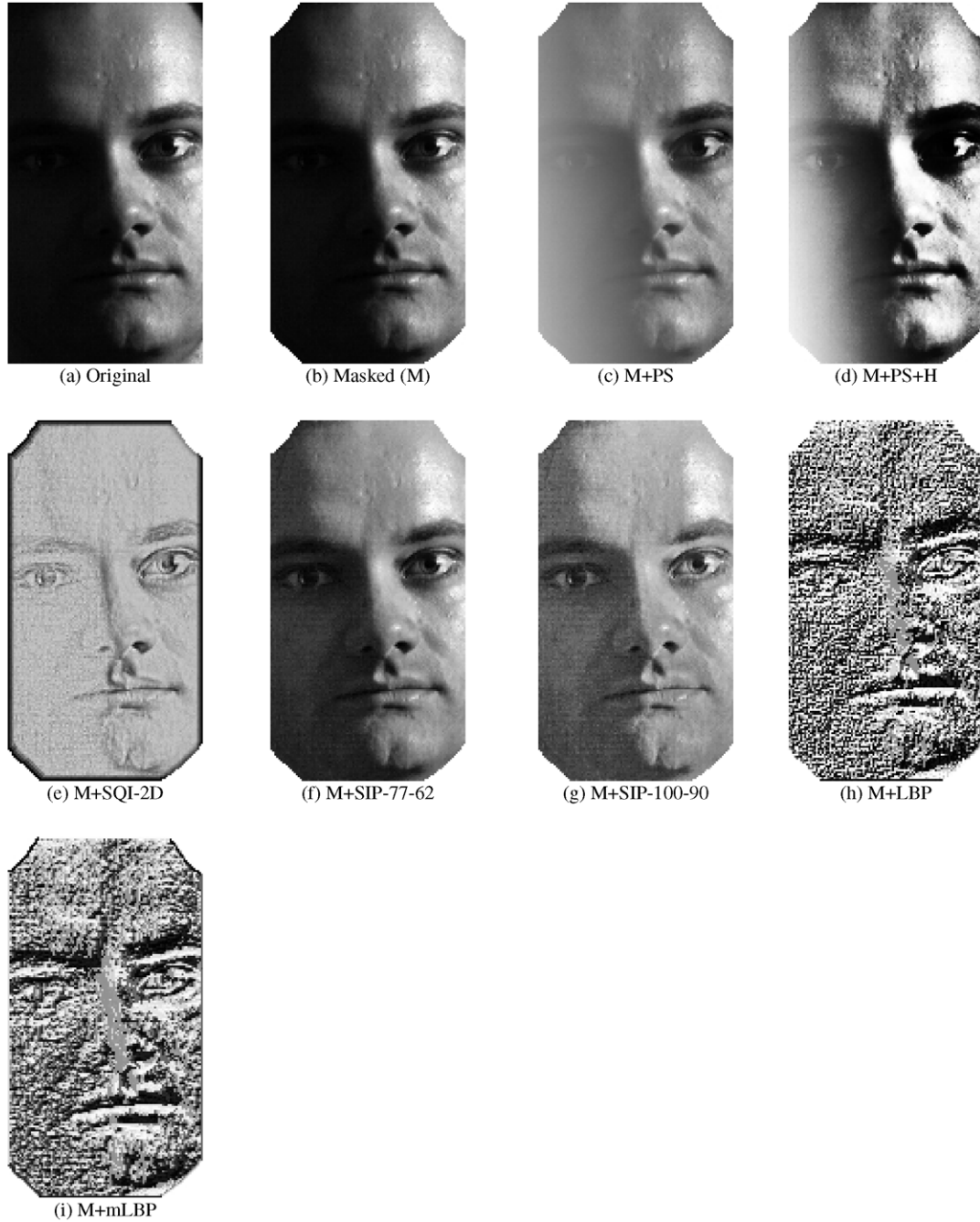
Fig. 2. Example image of an individual from the PIE database (a). The image is pre-processed by masking the central part (b). Afterwards several illumination invariant algorithms are applied (c–i). PS: illumination plane subtraction; HE: histogram equalization; SQI: self-quotient image; SIP: Gross and Brajovic' algorithm implemented by Shadow Illuminator Pro; LBP: local binary pattern; mLBP: modified LBP. See Section 3.2 for details.

It should be emphasized that in this work the LBP transform is applied just as a pre-processing step, which do not alter the face recognition methods to be employed (e.g., all images are LBP-transformed and then processed). In other works (e.g., Ahonen et al., 2004) spatial histograms of LBP features are computed, and then the recognition is carried out by measuring the histograms similarity using Chi square statistics, histogram intersection or Log-likelihood statistics.

2.5. Modified LBP

In the original formulation of LBP not all possible local structure kernels of a given neighborhood can be represented. This is mainly because the local differences are computed by comparing the neighborhood pixels with the center pixel, and obviously the center pixel cannot be compared with itself. This produce that in some cases LBP cannot capture correctly the local structure of the image area under analysis. For overcoming this drawback, the modified LBP (mLBP) (Fröba and Ernst, 2004) includes in the analysis the central pixel, by considering an enlarged neighborhood $N_1(x_c, y_c) = N(x_c, y_c) \cup I(x_c, y_c)$, and by comparing the pixels' intensity values against the local mean pixel intensity $\bar{I}(x, y)$ of all pixels in $N_1(x_c, y_c)$. Thus, the mLBP is defined as

$$mLBP(x, y) = \bigcup_{(x', y') \in N_1(x,y)} h(\bar{I}(x, y), I(x', y')) \tag{11}$$

mLBP transforms images in illumination invariant feature representations (see Figs. 1i and 2i), because all its computations are local,

and depend on the relative values between neighbor pixels (local contrast) and on the local mean pixels' intensity. In the case of a 3×3 neighborhood, mLBP(x,y) corresponds to the concatenation of nine bits.

3. Comparative study

The study is carried out in two stages. In the first stage, the five illumination compensation and normalization algorithms are compared and analyzed using a large amount of images from the PIE and Yale B databases, which contains face images with very different illumination conditions and a relative small number of individuals (10–68). As a result of these experiments, the algorithms with the best illumination compensation and normalization capabilities are selected for a deeper analysis. In the second stage, the selected algorithms are compared using the Notre Dame database. In this second set of experiments it is analyzed the performance of the algorithms when gallery and probe sets with a larger number of individuals are employed ($\sim$400). The statistical significance of the tests is also analyzed in the second stage.

3.1. Databases

The Yale B database contains 5760 single light source images of 10 individuals. Each individual is seen under 576 views conditions: nine different pose and 64 different illumination conditions (Georghiades et al., 2001). The database is divided into four different subsets according to the angle the light source direction forms with the camera axis. For our experiments we employ only frontal images (Pose 1). We use slightly different subsets than the original ones: Subset 1: up to 12° and 70 images, Subset 2 up to 30° and 120 images, Subset 3: up to 60° and 120 images, and Subset 4: up to 77° and 140 images. Subset 1 was used for building the eigenspace models (YALEB-1), and the other sets for testing (YALEB-2, YALEB-3 and YALEB-4).

The PIE (Pose, Illumination, and Expression) database contains a total of 41,368 images from 68 individuals, with different pose, illumination and expression conditions. The images were taken using the CMU 3D room using a set of 13 synchronized high-quality color cameras and 21 flashes (Sim et al., 2003). The images are classified into different sets depending on the including pose, illumination and expression variations. Regarding illumination conditions, PIE takes into account the fact that in the real world, illumination usually consists of an ambient light with perhaps one or two point sources. To obtain representative images of such cases PIE creators decided to capture images with the room lights on and with them off (Yale considers only this last case). We call the set of images with room lights on *lights*, and the set of images with room lights off *illum*. For our experiments we use only frontal images, which corresponds to the ones captured using camera *c27* (in the PIE terminology). From the *lights* set we select 24 images from 68 individuals (individuals 0–32, 34–37, and 39–69) totalizing 1632 images. The training set for the projection algorithms was built using images with good illumination conditions (frontal), which corresponds to images 00, 06, 08, 11 and 20 from each individual, totalizing 340 images. The remaining images form the test set (1,292 images). These sets correspond to our PIE-LIGHTS-TRAIN and PIE-LIGHTS-TEST sets. From the *illum* set we select 21 images from 67 individuals (individuals 0–32, 34–37, and 40–69) and 18 images from individual 39 (only 18 images are available for this individual), totalizing 1425 images. The eigenspace models are built using images with good illumination conditions (frontal), which correspond to images 08, 11 and 20 from each individual. In the case of individual 39 the images are the 06, 11 and 20 (this individual has no image 08). The total number of images used for

building the models is 204. The remaining images form the test set (1239 images). These sets correspond to our PIE-ILLUM-TRAIN and PIE-ILLUM-TEST sets.

In the University of Notre Dame Biometrics Database (Flynn et al., 2003) each subject was photographed with a high-resolution digital camera (1600×1200 or 2272×1704) under different lighting and expression conditions. Subjects were photographed every week for 10 weeks in the Spring of 2002, 13 weeks in the fall of 2002, and 15 weeks in the spring of 2003. The database defines the following conditions for faces: *fa* (normal expression), *fb* (smile expression), *lm* (three spotlights) and *lf* (two side spotlights). The following combinations of illumination and expression conditions are defined in collection B: *falm, fblm, falf* and *fblf*. As in (Chang et al., 2006) we use gallery and probe sets with images from the *falm, fblm, falf* and *fblf* illumination–expression pairs. We define six different gallery and six different probe sets. Each set is defined by the kind of images used for building these sets. Thus, a test set *falm–falf* means it was built using images from *falm* and *falf* for each individual. In each set we use two images per individual and 414 individuals. In the Notre Dame experiments use a generalized PCA model that does not depend on the gallery and probe set face images. This PCA model was built using 2152 face images obtained from other face databases and from Internet.

3.2. Test conditions

The algorithms are evaluated in a face identification scenario (1 against n comparison); face verification or watch-list search are not considered. Given the large number of results reported in this study, identification results are characterized in terms of rank-1 or top-1 recognition rates. Cumulative match characteristics (CMC) curves are not employed.

Before applying the illumination compensation and normalization algorithms other pre-processing stages are applied to obtain aligned face images of uniform size. First, faces are aligned by centering the eyes in the same relative positions, which should be at a fixed distance of 62 pixels. Then, the face area is cut from the image, and resized to 100×185 pixels. Examples of the obtained images are shown in Figs. 1a and 2a. Finally, face images are masked by cutting the image corners. Examples of this masked face images (M images) can be seen in Figs. 1b and 2b. The illumination invariant algorithms to be evaluated are (see explanation in Section 2):

- PS + HE: illumination plane subtraction (PS) applied jointly with histogram equalization (HE) was the pre-processing stage used in (Ruiz-del-Solar and Navarrete, 2005), which correspond to the comparative study of eigenspace-based face recognition algorithms that is being extended in the present work. For this reason PS + HE will be taken as the baseline algorithm for performing the comparisons.
- LBP: local binary pattern with a 3×3 pixels neighborhood.
- mLBP: modified LBP with a 3×3 pixels neighborhood.
- SIP-77-62 and SIP-100-90: Gross and Brajovic' algorithm implemented by the SIP (Shadow Illuminator Pro) software, Version 2.1.8, Build 234. The key parameters of the algorithm are *amount*, which specifies how much of the correction effect is applied to the original image, and *fill light*, which specifies how "flat" the illumination field is. After several tests we choose using two different combinations of parameters. In the SIP-77-62 case, the *amount* and *fill light* parameters are set to 77 and 62, respectively, while in the SIP-100-90 the parameters are set 100 and 90.
- SQI: self-quotient image (SQI) algorithm.

It is important to mention that in the case of the SQI and SIP algorithms, the parameters were hand tuned by us. After several experiments we selected the parameters that allowed us to obtain the highest recognition rate for each method. One drawback of these methods is their dependence of the parameters' values selection. We think that the algorithms should be robust enough for not depending largely on the parameters, which is not the case for SQI and SIP.

In the first stage of our study, the five algorithms under comparison were applied in 16 different face recognition systems, which are built using four different projections methods: PCA – (principal component analysis), FLD – (Fisher linear discriminant), KPCA – Kernel PCA (Gaussian–Kernel), and KFD – Kernel–Fisher discriminant (Gaussian kernel), and four different similarity measures: Euclidean-, Mahalanobis-, Cosines- and Whitening-Cosines-distance. These projection methods and similarity measures, as well as their corresponding training or modeling procedures, are detailed described in (Ruiz-del-Solar and Navarrete, 2005). In all cases the projection procedure consider intensity normalization of the face vectors (zero-mean and unit variance). In all experiments the number of projection axes employed in the FLD and KFD systems is equal to the number of classes minus one (9 axes in the case of Yale B and 67 axes in the case of PIE). In the PCA and KPCA systems the number of projection axes is the resulting of a *normalized residual mean square error* of 5% (Swets and Weng, 1996). We selected the two best performing algorithms to be further analyzed.

In the second stage of the study, we decided to use only PCA projections, given that: (i) the gallery sets contains just 1 or 2 images per individual, which makes very difficult to built a proper FLD or KFD representation, and (ii) the results obtained in stage one show that the pre-processing algorithms have a similar behavior in the PCA and kernel PCA representations. PCA was applied using the same four similarity measures: Euclidean-, Mahalanobis-, Cosines- and Whitening-Cosines-distance. In all experiments we fix the number of projection axes to 200. In addition, we employ the McNemar to determine whether one algorithm is significant better than the other.

3.3. Stage 1: Simulations using the Yale B and PIE databases

The first simulations were carried out using the Yale B database. The construction of the different recognition systems was carried out using the YALEB-1 subset, which contains seven images for each of the 10 database individuals. For each experiment we used a fixed number of images per individual for building the projection (e.g., PCA) space. Thus, experiments with 2, 3, 4, 5, 6 and 7 images per individual were carried out. In order to obtain statistical representative results, we took the average of several sets of experiments for each fixed number of training images. Because of space reasons, in this paper we just report the obtained results when using 2 and 7 images per class, which correspond to the most difficult identification scenario (2 images) and the most reported one for the Yale B database (7 images). The complete results using 2 to 7 images per class are reported in (Ruiz-del-Solar and Quinteros, 2006). In Tables 1 and 2 are displayed the results of the recognition experiments using subsets YALEB-2, YALEB-3 and YALEB-4, which contain 12, 12 and 14 images per individual respectively. For each of the 16 face recognitions systems and five different illumination compensation algorithms, the average top-1 recognition rate (first

Table 1
Yale B database: top-1 recognition rate (face identification scenario), 10 individuals, only frontal images (pose 1)

		M + PS + HE			M + LBP			M + mLBP			M + SIP1-77-62			M + SIP2-100-90			M + SQI		
		1 vs 2	1 vs 3	1 vs 4	1 vs 2	1 vs 3	1 vs 4	1 vs 2	1 vs 3	1 vs 4	1 vs 2	1 vs 3	1 vs 4	1 vs 2	1 vs 3	1 vs 4	1 vs 2	1 vs 3	1 vs 4
PCA	COS	100.00	96.58	52.07	99.75	99.83	91.93	100.00	99.92	94.79	99.08	94.17	64.71	98.17	96.42	76.79	96.00	99.25	95.71
		0.00	2.76	3.73	0.40	0.35	2.80	0.00	0.26	2.94	1.49	5.44	6.30	1.75	3.02	2.08	2.51	0.73	2.33
	EUC	100.00	96.58	52.00	99.75	95.50	81.93	99.67	98.75	90.29	99.08	94.50	65.00	98.00	95.92	76.71	95.58	98.83	95.21
		0.00	2.56	3.62	0.40	2.46	2.02	0.70	0.81	3.83	1.49	5.26	5.71	2.01	4.00	2.57	2.15	0.81	2.26
	WCOS	99.75	96.33	50.50	99.42	98.50	90.21	99.33	99.33	95.00	97.50	92.75	57.43	95.08	92.92	60.36	91.00	95.50	92.00
		0.79	3.58	6.00	0.56	2.32	6.88	0.35	0.66	3.43	2.58	5.63	6.79	3.52	3.25	14.70	2.60	1.05	3.01
	MAHA	100.00	95.25	48.57	77.50	61.33	33.50	91.17	86.00	47.29	98.92	94.58	57.21	97.17	93.00	58.71	93.33	96.92	92.36
		0.00	2.81	5.91	6.35	7.57	7.03	5.84	4.26	7.09	1.76	6.24	7.30	3.31	3.87	14.87	2.04	2.12	3.72
FLD	COS	100.00	95.08	51.50	100.00	99.50	88.50	99.83	99.42	90.71	97.42	87.83	58.93	94.17	83.17	62.71	89.33	88.83	88.71
		0.00	3.69	1.76	0.00	0.70	2.00	0.35	1.25	2.28	2.82	4.14	3.30	5.11	4.82	3.06	6.80	7.07	3.61
	EUC	99.75	93.75	47.21	98.50	96.58	76.21	98.83	98.25	87.00	97.42	87.08	57.86	92.08	77.08	58.36	84.75	87.00	85.57
		0.79	2.46	3.85	1.17	1.90	4.11	0.70	1.69	4.01	2.27	3.91	2.52	5.42	7.37	3.64	4.41	5.78	5.94
	WCOS	99.83	96.17	46.86	99.67	99.17	88.14	100.00	99.42	92.00	96.83	92.33	59.50	95.00	93.67	72.36	92.92	98.00	93.07
		0.53	2.49	1.97	0.43	0.96	2.41	0.00	0.88	2.56	3.06	6.54	7.02	3.89	3.60	13.69	3.45	1.58	2.21
	MAHA	100.00	94.83	47.86	99.83	99.75	87.57	99.92	99.42	89.36	98.42	93.83	61.71	98.17	94.33	75.21	97.42	99.67	96.43
		0.00	3.06	2.33	0.35	0.40	2.66	0.26	1.04	2.06	1.73	7.10	7.02	3.55	4.10	12.16	2.27	0.58	2.59
KPCA	COS	100.00	97.00	52.14	99.75	99.83	92.14	100.00	99.92	94.57	99.42	96.25	67.07	98.08	96.42	77.57	96.00	99.08	95.71
		0.00	2.81	3.70	0.40	0.35	2.95	0.00	0.26	2.76	1.04	2.97	3.29	1.89	2.99	2.52	2.51	0.61	2.33
	EUC	100.00	97.17	53.00	90.25	72.92	36.71	99.67	95.25	70.71	99.42	96.50	67.07	97.92	96.08	77.07	95.58	98.83	95.21
		0.00	2.05	3.75	2.72	10.92	8.17	0.70	3.24	6.06	1.04	2.42	3.52	2.16	3.56	3.00	2.15	0.81	2.43
	WCOS	100.00	97.33	55.79	99.67	99.58	93.79	99.67	99.92	96.00	98.17	96.17	62.86	95.42	93.75	62.50	91.75	95.92	92.07
		0.00	1.92	7.49	0.43	0.44	4.01	0.43	0.26	2.76	2.14	3.79	6.68	3.25	2.81	15.60	2.10	0.83	3.02
	MAHA	99.92	95.92	47.07	39.50	23.83	16.21	73.17	56.33	22.86	99.42	96.25	52.64	96.83	93.33	60.07	93.25	97.25	92.43
		0.26	2.73	3.11	11.11	7.01	3.88	10.84	9.85	7.89	1.25	3.85	8.50	3.44	4.75	16.10	1.78	2.29	3.60
KFD	COS	100.00	96.75	50.71	100.00	99.33	88.79	100.00	99.67	92.21	98.75	94.50	64.57	97.75	93.08	72.93	93.25	95.50	93.93
		0.00	2.50	3.53	0.00	0.77	1.88	0.00	0.70	2.77	2.70	2.40	2.29	2.12	4.21	4.71	4.15	3.87	2.78
	EUC	100.00	95.17	51.14	98.42	94.33	55.07	98.67	97.00	84.21	99.08	94.33	57.00	96.75	88.08	61.57	90.58	93.75	90.36
		0.00	3.06	3.27	0.61	3.06	12.87	0.58	1.68	4.93	1.73	2.83	2.20	2.82	4.27	3.76	3.56	3.97	3.54
	WCOS	100.00	93.33	46.00	79.08	65.92	29.50	92.17	78.25	39.64	99.00	89.25	58.00	95.75	90.75	68.93	91.67	96.92	92.71
		0.00	3.07	2.36	8.02	6.40	4.64	4.09	3.69	2.43	1.66	16.20	6.77	7.12	9.07	15.07	3.60	2.39	3.21
	MAHA	100.00	94.92	45.79	96.83	93.33	59.93	98.50	97.25	77.64	98.92	89.58	59.86	94.75	87.08	71.07	96.67	99.25	95.36
		0.00	3.27	5.28	2.63	4.55	9.06	1.51	0.79	8.32	1.42	19.97	6.61	7.53	16.50	17.53	2.69	1.39	2.90

Training using YALEB-1 subset, and 2 images per class. The average of 10 different training sets was considered (see explanation in main text). 1 vs *i* means training using YALEB-1 and test using YALEB-i.

Table 2
YaleB database: top-1 recognition rate (face identification scenario), 10 individuals, only frontal images (pose 1)

		M + PS + HE			M + LBP			M + mLBP			M + SIP1-77-62			M + SIP2-100-90			M + SQI		
		1 vs 2	1 vs 3	1 vs 4	1 vs 2	1 vs 3	1 vs 4	1 vs 2	1 vs 3	1 vs 4	1 vs 2	1 vs 3	1 vs 4	1 vs 2	1 vs 3	1 vs 4	1 vs 2	1 vs 3	1 vs 4
PCA	COS	100.00	99.17	57.86	100.00	100.00	95.00	100.00	100.00	99.29	100.00	100.00	67.14	100.00	100.00	75.00	99.17	100.00	97.86
		0.00	0.00	0.00	0.00	0.00	0.00	0.00	0.00	0.00	0.00	0.00	0.00	0.00	0.00	0.00	0.00	0.00	0.00
	EUC	100.00	99.17	57.86	100.00	99.17	92.14	100.00	100.00	98.57	100.00	100.00	67.14	100.00	100.00	75.00	99.17	100.00	97.86
		0.00	0.00	0.00	0.00	0.00	0.00	0.00	0.00	0.00	0.00	0.00	0.00	0.00	0.00	0.00	0.00	0.00	0.00
	WCOS	100.00	100.00	69.29	100.00	98.33	88.57	99.17	98.33	92.86	100.00	95.83	46.43	98.33	85.83	31.43	95.00	90.00	81.43
		0.00	0.00	0.00	0.00	0.00	0.00	0.00	0.00	0.00	0.00	0.00	0.00	0.00	0.00	0.00	0.00	0.00	0.00
	MAHA	100.00	100.00	62.86	78.33	71.67	47.86	88.33	86.67	64.29	100.00	95.83	50.00	95.83	85.00	30.71	88.33	88.33	75.00
		0.00	0.00	0.00	0.00	0.00	0.00	0.00	0.00	0.00	0.00	0.00	0.00	0.00	0.00	0.00	0.00	0.00	0.00
FLD	COS	100.00	98.33	53.57	100.00	100.00	93.57	100.00	100.00	92.86	100.00	96.67	69.29	100.00	97.50	75.71	98.33	99.17	98.57
		0.00	0.00	0.00	0.00	0.00	0.00	0.00	0.00	0.00	0.00	0.00	0.00	0.00	0.00	0.00	0.00	0.00	0.00
	EUC	100.00	99.17	52.86	98.33	96.67	86.43	99.17	99.17	95.71	100.00	97.50	71.43	99.17	94.17	75.00	100.00	100.00	100.00
		0.00	0.00	0.00	0.00	0.00	0.00	0.00	0.00	0.00	0.00	0.00	0.00	0.00	0.00	0.00	0.00	0.00	0.00
	WCOS	100.00	99.17	52.86	100.00	100.00	95.00	100.00	100.00	93.57	100.00	100.00	84.29	100.00	98.33	86.43	98.33	99.17	97.86
		0.00	0.00	0.00	0.00	0.00	0.00	0.00	0.00	0.00	0.00	0.00	0.00	0.00	0.00	0.00	0.00	0.00	0.00
	MAHA	100.00	97.50	50.00	100.00	100.00	95.00	100.00	100.00	90.71	100.00	100.00	75.71	100.00	99.17	85.00	100.00	100.00	98.57
		0.00	0.00	0.00	0.00	0.00	0.00	0.00	0.00	0.00	0.00	0.00	0.00	0.00	0.00	0.00	0.00	0.00	0.00
KPCA	COS	100.00	100.00	58.57	100.00	100.00	95.00	100.00	100.00	99.29	100.00	100.00	65.00	100.00	100.00	74.29	99.17	100.00	97.86
		0.00	0.00	0.00	0.00	0.00	0.00	0.00	0.00	0.00	0.00	0.00	0.00	0.00	0.00	0.00	0.00	0.00	0.00
	EUC	100.00	100.00	58.57	100.00	90.00	67.86	100.00	99.17	87.14	100.00	100.00	66.43	100.00	100.00	74.29	98.33	99.17	97.14
		0.00	0.00	0.00	0.00	0.00	0.00	0.00	0.00	0.00	0.00	0.00	0.00	0.00	0.00	0.00	0.00	0.00	0.00
	WCOS	100.00	100.00	82.14	100.00	99.17	95.00	100.00	99.17	97.14	100.00	99.17	67.86	98.33	85.83	34.29	95.00	90.83	81.43
		0.00	0.00	0.00	0.00	0.00	0.00	0.00	0.00	0.00	0.00	0.00	0.00	0.00	0.00	0.00	0.00	0.00	0.00
	MAHA	100.00	99.17	70.71	40.83	36.67	21.43	68.33	53.33	32.86	100.00	96.67	62.86	95.83	82.50	36.43	88.33	88.33	76.43
		0.00	0.00	0.00	0.00	0.00	0.00	0.00	0.00	0.00	0.00	0.00	0.00	0.00	0.00	0.00	0.00	0.00	0.00
KFD	COS	100.00	98.33	51.43	100.00	100.00	92.86	100.00	100.00	93.57	100.00	99.17	72.86	100.00	100.00	79.29	98.33	99.17	100.00
		0.00	0.00	0.00	0.00	0.00	0.00	0.00	0.00	0.00	0.00	0.00	0.00	0.00	0.00	0.00	0.00	0.00	0.00
	EUC	100.00	98.33	52.14	98.33	95.00	72.86	99.17	98.33	88.57	100.00	99.17	62.14	100.00	99.17	75.71	100.00	99.36	100.00
		0.00	0.00	0.00	0.00	0.00	0.00	0.00	0.00	0.00	0.00	0.00	0.00	0.00	0.00	0.00	0.00	0.00	0.00
	WCOS	100.00	97.50	48.57	90.00	70.83	39.29	96.67	85.00	59.29	100.00	96.67	75.71	100.00	99.17	83.57	94.17	97.50	97.14
		0.00	0.00	0.00	0.00	0.00	0.00	0.00	0.00	0.00	0.00	0.00	0.00	0.00	0.00	0.00	0.00	0.00	0.00
	MAHA	100.00	99.17	46.43	95.00	84.17	47.86	100.00	95.83	62.14	100.00	100.00	34.29	100.00	95.00	32.14	98.33	99.17	98.57
		0.00	0.00	0.00	0.00	0.00	0.00	0.00	0.00	0.00	0.00	0.00	0.00	0.00	0.00	0.00	0.00	0.00	0.00

Training using YALEB-1 subset, and seven images per class. 1 vs *i* means training using YALEB-1 and test using YALEB-i.

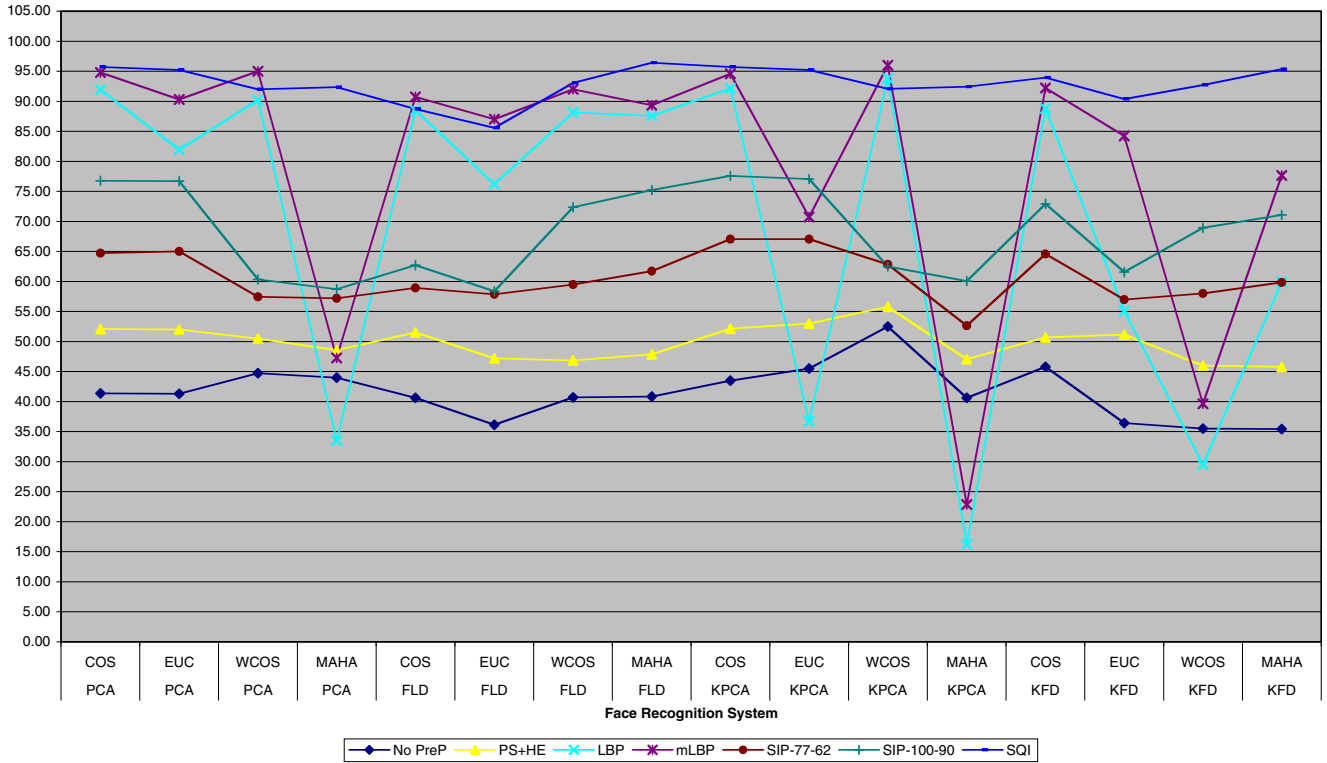**Fig. 3.** Yale B database: top-1 recognition rate (face identification scenario), 10 individuals, only frontal images (Pose 1). Training using YALEB-1 subset, and two images per class. The average of 10 different training sets was considered (see explanation in main text). Test using YALEB-4.

Table 3
PIE-ILLUM database: top-1 recognition rate (face identification scenario), 68 individuals, and training using two images per class

		M + PS + HE	M + LBP	M + mLBP	M + SIP1-77-62	M + SIP-100-90	M + SQI
PCA	COS	85.81	99.77	99.85	85.47	87.99	96.48
		0.04	0.09	0.04	0.50	0.48	0.00
	EUC	85.75	99.05	99.75	85.50	87.78	96.17
		0.00	0.18	0.00	0.45	0.59	0.09
	WCOS	87.73	99.43	99.80	90.22	93.33	93.37
		0.77	0.00	0.11	0.72	0.44	0.67
	MAHA	86.42	78.54	86.62	90.52	94.07	93.38
		0.22	2.24	2.82	0.76	0.29	0.31
FLD	COS	85.86	99.64	99.90	87.71	96.45	98.82
		1.90	0.04	0.04	0.06	2.27	0.27
	EUC	70.17	99.64	99.84	86.19	97.35	99.62
		3.15	0.04	0.00	1.42	1.90	0.04
	WCOS	85.86	99.64	99.90	87.71	96.45	98.82
		1.90	0.04	0.04	0.06	2.27	0.27
	WEUC	70.17	99.64	99.84	86.19	97.35	99.62
		3.15	0.04	0.00	1.42	1.90	0.04
KPCA	COS	86.88	78.67	85.77	90.71	94.09	93.76
		0.04	1.97	2.34	0.60	0.22	0.13
	EUC	86.11	77.26	84.14	89.50	90.37	93.14
		0.26	1.39	2.49	0.81	5.79	0.09
	WCOS	86.72	91.65	94.28	90.75	94.92	97.46
		0.15	1.12	0.22	0.79	0.55	0.00
	MAHA	85.90	72.12	79.00	87.86	86.00	91.74
		0.51	0.49	1.90	1.86	3.66	0.36
KFD	COS	86.54	94.14	96.10	90.01	95.20	97.18
		0.11	1.30	0.26	0.96	1.03	0.04
	EUC	86.78	99.13	99.56	89.50	96.38	99.18
		0.26	0.40	0.11	1.93	1.32	0.00
	WCOS	83.29	97.35	98.10	87.96	95.35	98.30
		0.18	0.72	0.33	1.51	1.79	0.13
	MAHA	85.72	99.13	99.56	88.01	96.40	99.30
		0.62	0.40	0.11	1.51	2.38	0.04

The average of three different training sets was considered (see explanation in main text).

row) and standard deviation (second row) are shown. By analyzing Tables 1 and 2 the first two obvious results are: (i) the top-1 recognition rate increases when the number of training images per class grows, and (ii) the recognition rate decreases when subsets YALEB-2, YALEB-3 and YALEB-4 are used, because between YALEB-2 and YALEB-4 increases the angle that the light source direction forms with the camera axis.

For analyzing the performance of the illumination compensation algorithms we will concentrate ourselves on the most difficult case: test set YALEB-4 and two images per class. In Fig. 3 are displayed the top-1 recognition rate for that case. The first interesting result is that the top-1 recognition rate increases from about 40% when no pre-processing is employed (*No Prep* case), to about 95% when the best performing pre-processing algorithms are applied. In most of the cases, the pre-processing algorithms increase the recognition rate. Second conclusion is that the highest recognition rates are obtained by SQI and mLBP, but SQI shows a high recognition rate in all cases while mLBP not. mLBP (as LBP) obtains poor results when the PCA–MAHA, KPCA–MAHA, KFD–MAHA and KFD–WCOS systems are employed. We do not have a clear explanation for this phenomenon, but one of the possible reasons is the fact that probably the whitening operation does not work properly in the mLBP (and LBP) domain, and that different similarity metrics (e.g., Hamming distances) should be used in these cases. The third best performing algorithm is LBP, which also shows a non-uniform behavior, followed by the two SIP variants. The baseline algorithm (PS + HE) shows the worse results, although the top-1 recognition rate is about 10% higher that the case when no pre-processing is employed.

Regarding the performance of the face recognition methods, for at least one pre-processing algorithm, each system achieves a very high top-1 recognition rate. When comparing the PCA-based systems with their KPCA-based counterparts we observe that the obtained results are similar. This is also the case when comparing

Fig. 4. PIE-ILLUM database: top-1 recognition rate (face identification scenario), 68 individuals, and training using two images per class. The average of three different training sets was considered (see explanation in main text).

Table 4
PIE-LIGHTS database: top-1 recognition rate (face identification scenario), 68 individuals and training using two images per class

		M+PS+HE	M+LBP	M+mLBP	M+SIP1-77-62	M+SIP-100-90	M+SQI
PCA	COS	99.92	100.00	100.00	99.90	99.17	99.87
		0.13	0.00	0.00	0.18	0.04	0.09
	EUC	99.97	99.95	99.97	99.90	99.15	99.87
		0.04	0.09	0.04	0.18	0.08	0.09
	WCOS	100.00	99.97	99.97	99.87	99.43	99.69
		0.00	0.04	0.04	0.22	0.92	0.08
	MAHA	99.92	97.96	98.84	99.87	99.59	99.82
		0.08	1.79	0.56	0.22	0.65	0.04
FLD	COS	99.82	100.00	100.00	99.02	92.05	98.92
		0.31	0.00	0.00	1.43	4.47	0.20
	EUC	99.54	100.00	100.00	99.12	91.87	98.84
		0.80	0.00	0.00	1.39	3.98	0.13
	WCOS	99.97	100.00	100.00	99.79	99.97	100.00
		0.04	0.00	0.00	0.09	0.04	0.00
	WEUC	99.92	100.00	100.00	99.69	99.90	100.00
		0.13	0.00	0.00	0.27	0.18	0.00
KPCA	COS	99.92	100.00	100.00	99.90	99.17	99.87
		0.13	0.00	0.00	0.18	0.09	0.09
	EUC	99.92	98.97	99.79	99.90	99.12	99.87
		0.13	0.04	0.12	0.18	0.12	0.09
	WCOS	100.00	99.97	100.00	99.77	99.36	99.79
		0.00	0.04	0.00	0.13	1.05	0.04
	MAHA	99.72	78.30	90.89	99.64	99.43	99.77
		0.36	11.44	5.16	0.09	0.98	0.00
KFD	COS	99.85	100.00	100.00	99.54	96.75	99.72
		0.27	0.00	0.00	0.54	1.90	0.12
	EUC	99.85	100.00	100.00	99.61	96.93	99.54
		0.27	0.00	0.00	0.54	1.47	0.15
	WCOS	99.97	99.92	99.87	99.74	99.87	99.95
		0.04	0.13	0.16	0.18	0.16	0.04
	MAHA	99.97	100.00	100.00	99.82	99.97	100.00
		0.04	0.00	0.00	0.18	0.04	0.00

The average of five different training sets was considered (see explanation in main text).

the results obtained with FLD and KFD. When comparing the similarity measures we can observe that using Cosines distance gives slightly better results than using Whitening-Cosines distance, and that using Euclidean distance gives slightly better results than using the Mahalanobis distance. These results are concordant with the ones obtained in (Ruiz-del-Solar and Navarrete, 2005), where a much more detailed analysis of the performance of these different recognition methods, in a uniform illumination scenario is presented.

In the second set of experiments we use the PIE *illum* and *lights* sets. In the *illum* set case the construction of the different recognition systems was carried out using the PIE-ILLUM-TRAIN subset, which contains three images for each of the 68 database individuals. For each experiment we used a fixed number of images per individual, 2 or 3, for building the PCA space. In this paper we just reported the obtained results for the most difficult identification scenario, two individuals. In order to obtain statistical representative results we take the average of several sets of experiments for each fixed number of training images. For testing purposes the subset PIE-ILLUM-TEST containing 18 images per individual (for individual 39 only 15 images) was employed. For each of the 16 face recognitions systems and 5 different illumination compensation algorithms, the average top-1 recognition rate (first row) and standard deviation (second row) are shown in Table 3. Results without standard deviation information are displayed in Fig. 4. Interestingly, in the case when no pre-processing is employed, the top-1 recognition rate varied largely from about 60% (PCA–COS, PCA–EUC, FLD–EUC and FLD–MAHA systems) to about 70% or more. When using pre-processing, the top-1 recognition rate increase to about 95% in each case (100% in some cases), for at least one-preprocessing algorithm. It can be observed that best results are obtained by the LBP and mLBP algorithms, except in the case of using PCA–MAHA and KPCA–MAHA. When using PCA–MAHA and KPCA–MAHA, best results are obtained by SIP-100-90 and SQI, respectively. However, if the results obtained by all recogni-
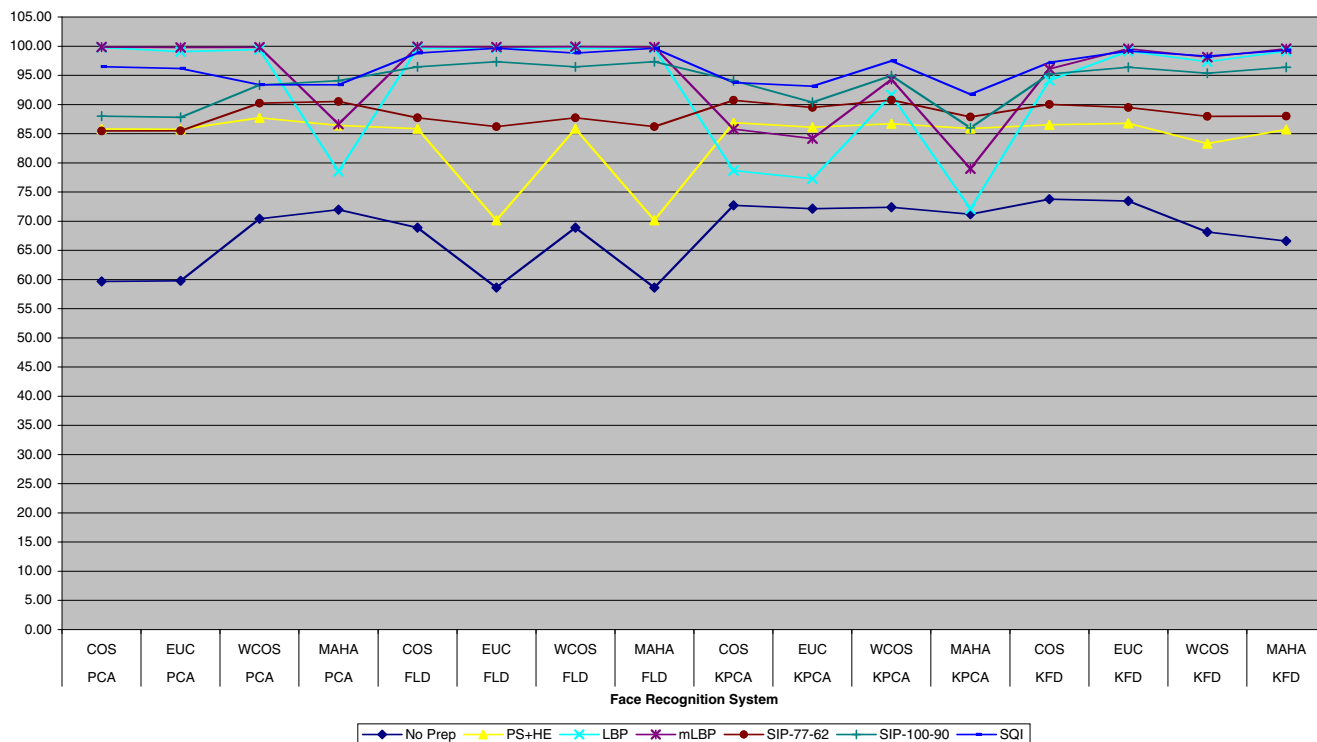
Fig. 5. PIE-LIGHTS database: top-1 recognition rate (face identification scenario), 68 individuals and training using two images per class. The average of five different training sets was considered (see explanation in main text).
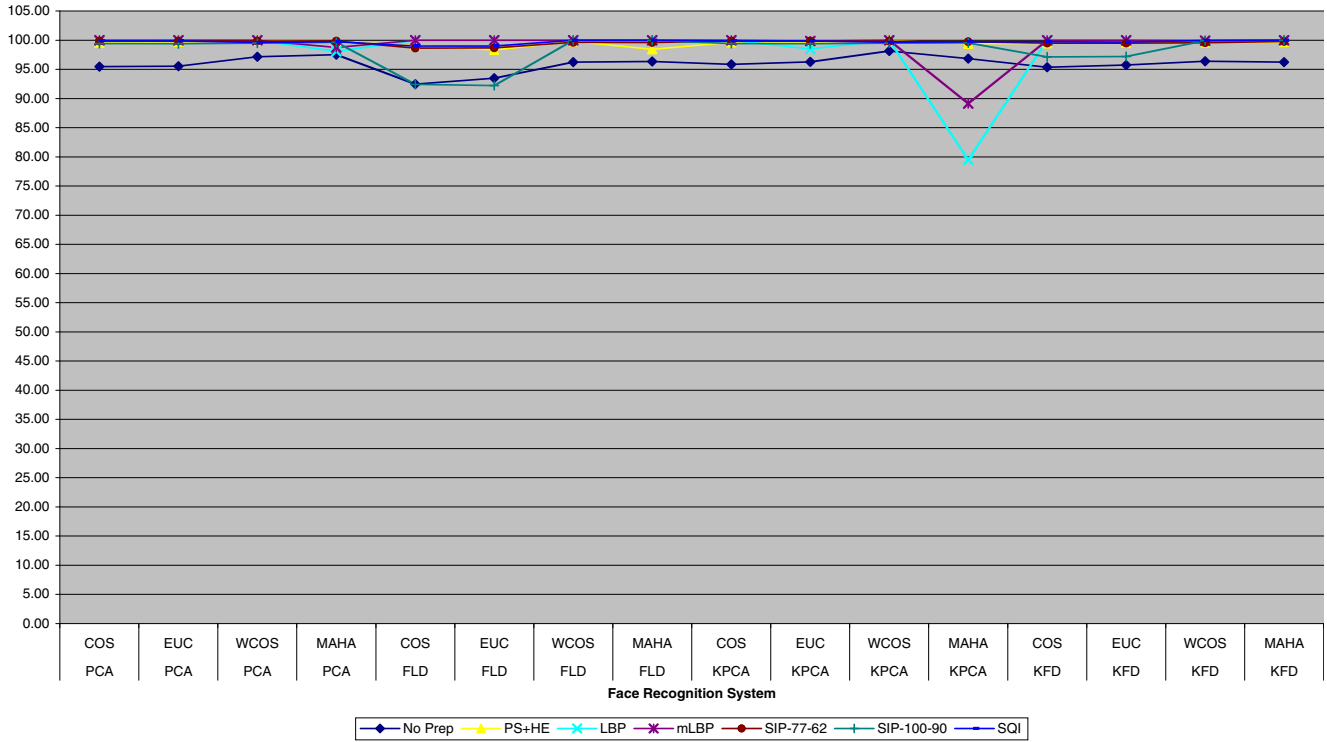
tion systems are taking into account, the third best performing algorithm is SQI; SIP-100-90 ranks fourth, and SIP-77-62 fifth. The baseline algorithm (PS + HE) shows the worse results, although

Table 5
Face identification comparisons of different methods

Methods	Error rate (%) corresponding to the top-1 recognition rate			
	Yale B			CMU PIE
	Subset 2	Subset 3	Subset 4	
Linear subspace for modeling illumination variation Georghiades et al. (2001)	0	0	15.0	–
Illumination cones-attached Georghiades et al. (2001)	0	0	8.6	–
Illumination cones-cast Georghiades et al. (2001)	0	0	0	–
Gradient angle Chen et al. (2000)	0	0	1.4	–
Harmonic images Zhang and Samaras (2003)	0	0.3	3.1	–
Illumination ratio images Zhao et al. (2003)	0	3.3	18.6	–
Quotient illumination relighting Shan et al. (2003)	0	0	9.4	–
9PL Lee et al. (2005)	0	0	0	1.9[b]
DCT in logarithmic domain Chen et al. (2006)	–	0	0.18	0.36
PCA-COS + mLBP	0	0	0.71	0.08/0[a]
PCA-EUC + mLBP	0	0	1.43	0.16/0[a]
FLD-EUC + SQI	0	0	0	6.06/0[a]
KFD-COS + SQI	0	0	0	2.46/0.21[a]
KFD-EUC + SQI	0	0	0	3.52/0[a]

In the case of the Yale B database the seven images from Subset 1 are used for modeling or building the subspaces. In the case of the CMU PIE database, depending on the employed subset, 3 or 5 images are used for modeling.
[a] In these cases the PIE sets *Illum/Lights* are considered.
[b] Seven images per class are employed for building the subspaces.

it improves the results obtained with no pre-processing, by increasing the top-1 recognition in more than 10%. In the case of the *lights* set, the construction of the different recognition systems was carried out using the PIE-LIGHTS-TRAIN subset, which contains five images for each of the 68 database individuals. For each experiment we used a fixed number of training images per individual, 2, 3, 4 or 5. In this paper we just reported the obtained results for the most difficult identification scenario, 2 individuals. In order to obtain representative results we take the average of several sets of experiments for each fixed number of training images. For testing purposes the subset PIE-ILLUM-TEST that contains 19 images per individual was used. For each of the 16 face recognitions systems and five different illumination compensation algorithms, the average top-1 recognition rate (first row) and standard deviation (second row) are shown in Table 4. Results without standard deviation information are displayed in Fig. 5.

An important aspect to notice is the fact that, the results obtained with the PIE *lights* set are better than the ones obtained with the *illum* set. The reason seems to be that in the *lights* set, images include room lights, which facilitate obtaining illumination compensation, because these images look more similar to images with uniform illumination, and they contain less intensive shadows. The images contained in the PIE *illum* and Yale B sets do not contain room lights, and therefore are harder to analyze. Another important result is the fact that for illumination compensation algorithms the Yale B Subset 4 (YALEB-4) is a harder benchmark than the PIE *illum* or *lights* sets. The reason is the large angle (>60°) that the light source direction forms with the camera axis, and the fact that no room lights are included.

In summary, by analyzing the simulations carried out using the Yale B and PIE databases we conclude that some of the compared algorithms achieve very high recognition rates when used as a pre-processing stage of standard eigenspace-based face recognition systems. This is the case of the mLBP and SQI algorithms.

In addition, it is interesting to analyze how is the performance of those algorithms when compared with others algorithms not

considered in this study. In Table 5 is compared the performance obtained by 11 of the best performing algorithms reported in the literature in the Yale B and CMU PIE databases, with the performance of our best performing algorithms. Five of those algorithms corresponds to face modeling approaches: *linear subspace for modeling illumination variation, illumination Cones-attached, illumination Cones-cast, harmonic images* and *9PL*, two correspond to normalization and preprocessing approaches derived from the QI method: *illumination ratio images* and *quotient illumination relighting*, and two correspond to invariant features extraction approaches: *gradient angle* and *DCT in Logarithmic Domain*. Nevertheless, it is important to remark that this comparison (Table 5) should be taken just as a reference, because not all algorithms have been tested in equal working conditions, because different groups have implemented them. In a near future we would like to implement some of these algorithms for having a more objective comparison. From Table 5 we can see that in terms of performance the best results are obtained by *illumination Cones-cast, 9PL, DCT in Logarithmic Domain*, and five of our algorithms: PCA − COS + mLBP, PCA − EUC + mLBP, FLD − EUC + SQI, KFD − COS + SQI and KFD − EUC + SQI. If we just

Table 6
Processing time of different algorithms applied to a 640 × 480 pixels image from the Yale B database *M* process includes alignment, resizing and masking

Algorithm	Time (ms)
M	0.11
M+PS+HE	1.93
M+LBP	4.65
M+mLBP	5.54
M+SIP-77-62	900[a]
M+SIP-100-90	900[a]
M+SQI-2D	354.23
M+SQI-1D	165.44

All algorithms were implemented by the authors (see details in main text), except SIP, in which case a commercial program was employed.

[a] Time obtained by a commercial program.

Table 7
Notre Dame database: top-1 recognition rate (face identification scenario), 414 individuals

		mLBP						SQI					
		falf-falm	falm-fblm	falf-fblm	falm-fblf	falf-fblf	fblf-fblm	falf-falm	falm-fblm	falf-fblm	falm-fblf	falf-fblf	fblf-fblm
falf-falm	PCA-COS	(+) 67.87	55.19	58.94	56.76	59.42	38.41	57.25	52.66	51.81	55.07	54.47	47.34
falf-falm	PCA-EUC	(+) 68.00	55.19	59.18	56.88	59.42	38.77	57.37	52.66	52.05	55.07	54.59	47.34
falf-falm	PCA-WCOS	(+) 65.22	52.29	56.76	53.62	57.73	33.33	54.83	48.67	49.88	48.79	49.40	38.89
falf-falm	PCA-MAHA	(+) 66.06	51.69	58.21	53.02	58.21	33.45	54.59	48.19	49.40	48.91	48.91	38.04
falf-falm	FLD-COS	(+) 66.55	(+) 53.50	(+) 58.82	(+) 54.59	(+) 59.18	37.44	45.77	38.77	43.60	45.41	44.57	39.25
falf-falm	FLD-EUC	(+) 61.47	(+) 49.03	(+) 54.47	(+) 49.40	53.14	34.54	48.07	39.25	43.84	45.77	45.77	39.49
falf-falm	FLD-WCOS	17.03	13.41	9.18	4.47	8.82	5.68	(+) 37.32	(+) 34.30	(+) 35.51	(+) 33.45	(+) 35.39	(+) 26.81
falf-falm	FLD-MAHA	18.96	15.58	11.96	6.76	11.84	6.88	(+) 28.62	(+) 26.33	(+) 23.91	(+) 24.15	(+) 24.28	(+)20.17
falm-fblm	PCA-COS	56.52	57.85	60.14	60.63	62.44	54.23	56.52	54.47	56.28	57.97	59.06	56.40
falm-fblm	PCA-EUC	56.52	57.97	60.39	60.87	62.32	54.11	56.76	54.47	56.52	57.97	59.30	56.40
falm-fblm	PCA-WCOS	49.52	53.38	56.64	55.19	57.97	48.91	51.81	51.09	52.54	53.86	55.19	49.76
falm-fblm	PCA-MAHA	50.97	53.26	56.64	54.71	57.85	49.03	50.72	50.48	51.81	53.86	54.35	49.15
falm-fblm	FLD-COS	(+) 55.56	(+) 55.07	(+) 57.97	(+) 59.42	(+) 61.35	(+) 52.90	42.27	38.53	44.69	46.86	49.64	48.91
falm-fblm	FLD-EUC	(+) 51.81	(+) 50.00	53.50	(+) 52.29	(+) 55.92	46.62	45.53	40.82	46.50	48.07	50.48	49.03
falm-fblm	FLD-WEUC	11.59	12.68	10.02	5.07	9.90	10.99	(+) 36.47	(+) 36.11	(+) 36.35	(+) 38.29	(+) 41.30	(+) 35.99
falm-fblm	FLD-MAHA	13.77	14.98	12.92	8.21	13.04	13.89	(+) 27.78	(+) 26.93	(+) 27.42	(+) 28.86	(+) 32.13	(+) 29.47
falf-fblm	PCA-COS	54.35	58.70	59.42	59.66	60.99	56.16	54.83	57.13	54.47	59.90	57.49	57.13
falf-fblm	PCA-EUC	54.47	58.82	59.90	59.78	60.87	56.16	54.95	57.13	54.47	59.90	57.61	57.13
falf-fblm	PCA-WCOS	49.28	54.95	57.37	56.40	58.21	49.64	48.91	51.21	50.48	53.38	52.66	50.48
falf-fblm	PCA-MAHA	50.36	54.47	57.85	(+) 55.80	(+) 55.80	48.91	49.03	50.85	50.24	52.78	52.29	49.52
falf-fblm	FLD-COS	(+) 53.74	(+) 55.43	(+) 58.33	(+) 58.70	(+) 58.70	(+) 55.80	41.91	41.55	44.32	48.79	48.07	48.79
falf-fblm	FLD-EUC	(+) 49.28	50.72	51.93	(+) 53.62	(+) 53.62	49.76	43.60	42.63	43.96	49.40	49.40	48.91
falf-fblm	FLD-WCOS	11.71	13.77	9.78	6.16	9.06	12.80	(+) 37.32	(+) 38.77	(+) 36.35	(+) 40.34	(+) 40.94	(+) 38.16
falf-fblm	FLD-MAHA	14.37	16.55	13.04	9.90	12.32	15.70	(+) 26.69	(+) 28.86	(+) 25.97	(+) 29.35	(+) 28.86	(+) 29.83
falm-fblf	PCA-COS	57.25	61.47	63.77	(+) 60.99	63.41	55.31	55.43	55.68	57.00	55.19	56.64	55.31
falm-fblf	PCA-EUC	57.37	61.35	63.53	(+) 60.99	63.29	55.68	55.56	55.68	57.25	55.19	56.76	55.31
falm-fblf	PCA-WCOS	49.76	55.56	59.90	53.26	57.85	50.60	50.97	53.50	54.95	50.24	52.42	50.72
falm-fblf	PCA-MAHA	50.72	55.92	59.90	53.62	56.76	50.97	50.00	53.02	53.86	50.97	51.57	50.36
falm-fblf	FLD-COS	(+) 55.92	(+) 58.94	(+) 61.35	(+) 59.54	(+) 61.71	(+) 53.74	40.82	40.10	46.50	44.44	44.93	47.34
falm-fblf	FLD-EUC	52.78	52.90	58.45	51.45	55.31	48.43	44.08	42.15	48.07	46.14	46.86	47.58
falm-fblf	FLD-WCOS	12.68	15.22	11.59	4.83	9.66	13.04	(+) 35.14	(+) 38.04	(+) 40.70	(+) 33.09	37.92	(+) 35.75
falm-fblf	FLD-MAHA	13.77	17.39	14.98	6.88	12.32	14.25	(+) 27.42	(+) 29.47	(+) 30.56	(+) 24.64	(+) 28.74	(+) 28.26
falf-fblf	PCA-COS	55.07	62.32	63.04	60.02	61.96	57.25	53.74	58.33	55.19	57.13	55.07	56.04
falf-fblf	PCA-EUC	55.31	62.20	63.04	59.90	61.84	57.73	53.74	58.33	55.19	57.13	55.07	56.04
falf-fblf	PCA-WCOS	49.52	57.13	60.63	54.47	58.09	51.33	48.07	53.62	52.90	49.76	49.88	51.45
falf-fblf	PCA-MAHA	(+) 50.12	57.13	(+) 61.11	54.71	57.00	50.85	48.31	53.38	52.29	49.88	49.52	50.72
falf-fblf	FLD-COS	(+) 54.11	(+) 59.30	(+) 61.71	(+) 58.82	(+) 61.23	(+) 56.64	40.46	43.12	46.14	46.38	43.36	47.22
falf-fblf	FLD-EUC	50.24	53.62	56.88	52.78	(+) 53.14	51.57	42.15	43.96	45.53	47.46	45.77	47.46
falf-fblf	FLD-WCOS	12.80	16.30	11.35	5.92	8.82	14.86	(+) 35.99	(+) 40.70	(+) 40.70	(+) 35.14	(+) 37.56	(+) 37.92
falf-fblf	FLD-MAHA	14.37	18.96	15.10	8.57	11.59	16.06	(+) 26.33	(+) 31.40	(+) 29.11	(+) 25.12	(+) 25.48	(+) 28.62
fblf-fblm	PCA-COS	43.72	64.98	64.25	63.89	64.98	(+) 73.07	(+) 53.02	60.14	59.66	60.02	59.66	65.10
fblf-fblm	PCA-EUC	43.84	64.98	64.25	63.89	64.73	(+) 73.07	(+) 53.14	60.14	59.66	60.02	59.78	65.10
fblf-fblm	PCA-WCOS	33.82	58.21	60.51	56.04	58.33	66.91	(+) 45.05	56.04	55.56	54.83	55.68	62.32
fblf-fblm	PCA-MAHA	35.02	58.70	59.54	56.40	56.64	66.43	44.44	55.68	54.71	54.83	54.95	61.84
fblf-fblm	FLD-COS	43.12	60.87	60.87	(+) 63.65	(+) 63.41	(+) 72.10	36.96	42.87	47.22	47.83	48.43	56.88
fblf-fblm	FLD-EUC	40.58	54.59	55.92	55.68	55.92	63.65	39.61	45.53	48.19	49.76	50.48	57.00
fblf-fblm	FLD-WCOS	7.37	15.58	12.20	6.52	9.90	20.17	(+) 35.14	(+) 42.51	(+) 41.55	(+) 39.98	(+) 43.48	(+) 47.10
fblf-fblm	FLD-MAHA	9.18	18.36	16.06	10.02	12.80	23.07	(+) 25.48	(+) 32.00	(+) 32.61	(+) 29.83	(+) 33.33	(+) 37.92

Results are displayed for the mLBP and SQI algorithms. In each case, columns refer to different gallery sets. Rows refer to different combinations of probe sets and face recognition systems. (+) means that one algorithm (mLBP or SQI) outperforms the other one according to the McNemar test.

consider the Yale B results (some of the compared algorithms do not have results for the PIE database), best performing algorithms are *illumination Cones-cast*, *9PL*, FLD – EUC + SQI, KFD – COS + SQI and KFD – EUC + SQI. However, it should be considered that *illumination Cones-cast* and *9PL* are face modeling methods, and that for this reason they require more training or modeling images. On the other hand, from the algorithms that have reported results in Yale B and PIE we observe that best results are obtained by PCA – COS + mLBP and PCA – EUC + mLBP, which show also the highest recognition rates in the PIE database.

The processing time is another important aspect that should be considered when comparing algorithms. We analyzed the processing time of the five algorithms under comparison. The experiments were performed in a standard PC (Intel Pentium 4, 2.60Ghz, 256MB RAM) with Linux Debian, kernel 2.6.8-2-686, and an image of 640×480 pixels from the Yale B database was processed. In the case of the SIP program, Windows XP Professional Edition with Service Pack 2 was employed. In the case of SQI we have two different implementations: in the SQI-2D case the 2D Gaussian filters are implemented using 2D windows, but in the SQI-1D the same filters are implemented using 1D windows. The obtained results are shown in Table 6. We can observe that PS + HE is the fastest algorithm, but as we have already seen, the one with the worst performance. LBP and mLBP are also very fast, with a processing time of 5–6 ms. These two algorithms are followed at a large distance by SQI. In fact the SQI algorithm is between 30 and 70 times slower than LBP and mLBP, depending on the employed implementation (2D or 1D filters). The SIP is a special case because we do not employ our own implementation of the algorithm, but a commercial program that implements it, and also a different Operation System (Windows instead of Linux). In any case we can affirm that after our estimations SIP is slower than LBP and mLBP.

It should be mentioned that although these absolute number (processing time in ms) could change depending on the implementation (e.g., employed PC), they show a tendency: PS + HE, LBP and mLBP are very fast, and SIP and SQI are slower. A last advantage of LBP and mLBP is the fact of being almost parameter free (the default window size is 3×3 pixels). This is not the case of SQI or SIP, where several parameters should be tuned, affecting the final performance of these methods. PS + HE has no parameters but a low performance.

As a result of the analyzed experiments we selected the mLBP and SQI algorithms to be further analyzed in stage 2.

3.4. Stage 2: Simulations using the Notre Dame database

The mLBP and SQI are further analyzed in a more natural scenario using the Notre Dame Database. We define six gallery and six probe sets that correspond to different illumination-expression conditions (see explanation in Section 3.1). In each experiment the sets contains 414 individual and two images per individual. Table 7 shows the results of all 36 experiments in terms of recognition rate. mLBP and SQI are compared using the McNemar test. We consider that one of the algorithms outperforms the other when the probability of the null hypothesis (both algorithms performs the same) is smaller than 0.001. In Table 7 "(+)" means that one algorithm outperforms the other in the McNemar test.

By analyzing the obtained results it can be seen that when using the FLD–WCOS and FLD–MAHA projection methods SQI always outperforms the mLBP algorithm. However, for most of the other projection methods mLBP outperforms SQI. It can be also seen that for a given gallery and probe set (e.g., *falf–falm* with *falm-fblm*) in most of the cases the best performing recognition system is achieved using the mLBP as a pre-processing algorithm.

4. Conclusions

Variable illumination is a major problem in face recognition. The aim of this work was to investigate it by carrying out an independent comparative study among several illumination compensation and normalization algorithms. We concentrated ourselves in algorithms with the following properties: (i) general purpose, (ii) no modeling steps or training images required, (iii) simplicity, (iv) high speed, and (v) high performance in terms of recognition rates. Thus, five different algorithms were compared by using each of them as a pre-processing stage in 16 different eigenspace-based face recognition systems. The compared algorithms were: PS + HE (plane subtraction + histogram equalization), LBP (local binary pattern), mLBP (modified LBP), SQI (self-quotient image) and the Gross and Brajovic' preprocessing algorithm. It is important to notice that all compared algorithms, with the exception of the baseline algorithm (PS + HE), are based on local computations that depend on the relative values between neighbor pixels and/or the local mean pixels' intensity. This allows obtaining very good results in terms of illumination compensation and normalization.

The experiments were carried out using the Yale B, PIE and Notre Dame databases in a face identification scenario with large variations in illumination. From these experiments we can conclude that when using an eigenspace-based face recognition system and a proper illumination compensation and normalization algorithm, having at least two example images with uniform illumination per individual is enough for obtaining high top-1 recognition rates. Best results were obtained by the SQI and mLBP algorithms. When both algorithms are compared using a test of statistical significance (McNemar test) with different face recognition systems, in most of the cases mLBP outperforms SQI. In addition, mLBP has a high processing speed and it is almost parameter free (the default window size is 3×3 pixels). In the reported experiments, LBP and SIP obtains also good results, but these results are not as good as the ones obtained by mLBP and SQI.

A problem to be tacked in the near future is the fact that LBP and mLBP do not work properly when using similarity measures that use whitening (Mahalanobis- and Whitening-Cosines distance). Probably the whitening operation does not work properly in the LBP and mLBP domains, and different similarity metrics (e.g., Hamming distances) should be used in these cases. We are currently analyzing this issue.

In a second line of work, we would like to extend our comparative study by including other recently proposed illumination compensation algorithms as for example the *DCT in Logarithmic Domain* algorithm. In this case it should be analyzed how to select the proper number of DCT coefficients for a given image size and target cutoff frequency.

References

Adini, Y., Moses, Y., Ullman, S., 1997. Face recognition: The problem of compensating for changes in illumination direction. IEEE Trans. Pattern Anal. Machine Intell. 19 (7), 721–732.

Ahonen, T., Hadid, A., Pietikainen, M., 2004. Face recognition with local binary patterns. Lecture Notes Comput. Sci. 3021 (ECCV 2004), 469–481.

Basri, R., Jacobs, D., 2004. Illumination modeling for face recognition. In: Li, Stan Z., Jain, Anil K. (Eds.), Handbook of Face Recognition. Springer-Verlag (Chapter 5).

Belhumeur, P., Kriegman, D., 1998. What is the set of images of an object under all possible illumination conditions. Internat. J. Comput. Vision 28 (3), 245–260.

Chang, K.I., Bowyer, K.W., Flynn, P.J., 2006. An evaluation of multimodal 2D + 3D face biometrics. IEEE Trans. Pattern Anal. Machine Intell. 27 (4), 619–624.

Chen, H., Belhumeur, P., Kriegman, D., 2000. In search of illumination invariants. In: Proc. IEEE Conf. Computer Vision and Pattern Recognition, vol. 1, 2000, pp. 13–15.

Chen, W., Joo Er, M., Wu, S., 2006. Illumination compensation and normalization for robust face recognition using discrete cosine transform in logarithmic domain. IEEE Trans. Systems, Man, Cybernetics B 36 (2), 458–466.

Flynn, P.J., Bowyer, K.W., Phillips, P.J., 2003. Assessment of time dependency in face recognition: An initial study. Audio Video-Based Biometric Person Authenticat., 44–51.

Fröba, B., Ernst, A., 2004. Face detection with the modified census transform. In: Proc. sixth Internat. Conf. on Face and Gesture Recognition – FG 2004, 91–96, Seoul, Korea, May 2004.

Georghiades, A., Belhumeur, P., Kriegman, D., 2001. From few to many: Illumination cone models for face recognition under variable lighting and pose. IEEE Trans. Pattern Anal. Machine Intell. 23 (6), 643–660.

Gross, R., Baker, S., Matthews, I., Kanade, T., 2004. Face recognition across pose and illumination. In: Li, Stan Z., Jain, Anil K. (Eds.), Handbook of Face Recognition. Springer-Verlag (Chapter 9).

Gross, R., Brajovic, V., 2003. An image preprocessing algorithm for illumination invariant face recognition. In: Proc. fourth Internat. Conf. on Audio- and Video-based Biometric Person Authentication – AVBPA 2003, 10–18, Guildford, UK.

Jobson, D., Rahman, Z., Woodell, G., 1996. Retinex image processing: Improved fidelity to direct visual observation. In: Proc. IS& T/SID Fourth Color Imaging Conf.: Color Science, Systems and Applications, Nov., pp. 124–126.

Land, E.H., 1977. The retinex theory of color vision. Sci. Amer. 237 (6), 108–128.

Lee, K.-C., Ho, J., Kriegman, D., 2005. Acquiring linear subspaces for face recognition under variable lighting. IEEE Trans. Pattern Anal. Machine Intell. 27 (5), 684–698.

Ojala, T., Pietikainen, M., Harwood, D., 1996. A comparative study of texture measures with classification based on features distributions. Pattern Recognition 29 (1), 51–59.

PIE Database. <http://www.ri.cmu.edu/projects/project_418.html>.

Phillips, J., Scruggs, T., O'Toole, A., Flynn, P., Bowyer, K., Schott, C., Sharpe, M., 2007. FRVT 2006 and ICE 2006 large-scale results. NISTIR 7408 Report, March 2007.

Pizer, S., Amburn, E., Austin, J., et al., 1987. Adaptive histogram equalization and its variations. Computer, Vision Graphics, Image Process. 39 (3), 355–368.

Ramamoorthi, R., 2002. Analytic PCA construction for theoretical analysis of lighting variability in images of a Lambertian object. IEEE Trans. Pattern Anal. Machine Intell. 24 (10), 1322–1333.

Ruiz-del-Solar, J., Navarrete, P., 2005. Eigenspace-based face recognition: A comparative study of different approaches. IEEE Trans. Systems, Man, Cybernetics C 35 (3), 315–325.

Ruiz-del-Solar, J., Quinteros, J., 2006. Comparing pre-processing approaches for illumination invariant face recognition. Technical Report UCH-DIE-VISION-2006-04, Dept. Elect. Eng., Universidad de Chile. <http://vision.die.uchile.cl/>.

Shan, S., Gao, W., Cao, B., Zhao, D., 2003. Illumination normalization for robust face recognition against varying lighting conditions. In: Proc. IEEE Workshop on AMFG, pp. 157–164.

Shin, D., Lee, H.-S., kim, D., 2008. Illumination-robust face recognition using ridge regressive bilinear models. Pattern Recognition Lett. 29, 49–58.

Shashua, A., Riklin-Raviv, T., 2001. The quotient image: Class based re-rendering and recognition with varying illuminations. IEEE Trans. Pattern Anal. Machine Intell. 23 (2), 129–139.

Short, J., Kittler, J., Messer, K., 2004. A comparison of photometric normalisation algorithms for face verification. In: Proc. sixth Internat. Conf. on Face and Gesture Recognition – FG 2004, Seoul, Korea, pp. 254–259.

Sim, T., Baker, S., Bsat, M., 2003. The CMU pose, illumination, and expression database. IEEE Trans. Pattern Anal. Machine Intell. 25 (12), 1615–1618.

Sung, K., Poggio, T., 1998. Example-based learning for viewed-based human face detection. IEEE Trans. Pattern Anal. Machine Intell. 20 (1), 39–51.

Swets, D., Weng, J., 1996. Using discriminant eigenfeatures for image retrieval. IEEE Trans. Pattern Anal. Machine Intell. 18 (8), 831–836.

Turk, M., Pentland, A., 1991. Eigenfaces for recognition. J. Cognit. Neurosci. 3 (1), 71–86.

Wang, H., Li, S., Wang, Y., 2004. Face recognition under varying lighting conditions using self quotient image. In: Proc. 6th Internat. Conf. on Face and Gesture Recognition – FG 2004, Seoul, Korea, May 2004, pp. 819–824.

Xie, X., Lam, K.-M., 2006. An efficient illumination normalization method for face recognition. Pattern Recognition Lett. 27, 609–617.

Yale Face Database B. <http://cvc.yale.edu/projects/yalefacesB/yalefacesB.html>.

Zabih, R., Woodfill, J., 1994. Non-parametric local transforms for computing visual correspondence. In: Proc. 3rd European Conf. on Computer Vision – ECCV, vol. II, Stockholm, Sweden, pp. 151–158.

Zhang, L., Samaras, D., 2003. Face recognition under variable lighting using harmonic image exemplars, In: Proc. IEEE Conf. Computer Vision and Pattern Recognition, vol. 1, 2003, pp. 19–25.

Zhang, L., Wang, S., Samaras, D., 2005. Face synthesis and recognition from a single image under arbitrary unknown lighting using a spherical harmonic basis Morphable model. In: Proc. Internat. Conf. on Computer Vision and Pattern Recognition – CVPR 2005, vol. 2, June 20–25, San Diego, USA, pp. 209–216.

Zhao, J., Su, Y., Wang, D., Luo, S., 2003. Illumination ratio image: Synthesizing and recognition with varying illuminations. Pattern Recognition Lett. 24, 2703–2710.